

# A High-Pressure Infrared Spectroscopic Study on the Interaction of Ionic Liquids with PEO-PPO-PEO Block Copolymers and 1,4-Dioxane

Jyh-Chiang Jiang,<sup>†</sup> Sz-Chi Li,<sup>‡</sup> Pao-Ming Shih,<sup>‡</sup> Tzu-Chieh Hung,<sup>‡</sup> Shu-Chieh Chang,<sup>‡</sup> Sheng Hsien Lin,<sup>§,⊥</sup> and Hai-Chou Chang<sup>\*,‡</sup>

<sup>†</sup>Department of Chemical Engineering, National Taiwan University of Science and Technology, Taipei 106, Taiwan

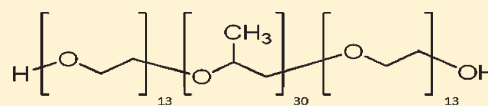
<sup>‡</sup>Department of Chemistry, National Dong Hwa University, Shoufeng, Hualien 974, Taiwan

<sup>§</sup>Department of Applied Chemistry, National Chiao Tung University, Hsinchu 30010, Taiwan

<sup>⊥</sup>Institute of Atomic and Molecular Sciences, Academia Sinica, P.O. Box 23-166, Taipei 106, Taiwan

**S** Supporting Information

**ABSTRACT:** We have investigated the effect of pressure on imidazolium C—H—O interactions in 1-ethyl-3-methylimidazolium bis(trifluoromethylsulfonyl)amide (EMI<sup>+</sup>TFSA<sup>−</sup>)/L64 and EMI<sup>+</sup>TFSA<sup>−</sup>/1,4-dioxane mixtures. The addition of Pluronic L64 to EMI<sup>+</sup>TFSA<sup>−</sup> leads to appreciable changes in band frequencies and shapes of the imidazolium C—H stretching bands. A possible explanation is the formation of C—H—O interactions between imidazolium C—H groups and oxygen atoms of polyethylene oxides (PEOs). In other words, L64 can be added to change the relative contribution of the isolated and associated components of EMI<sup>+</sup>TFSA<sup>−</sup>. In contrast to L64, the oxygen atoms of 1,4-dioxane cannot perturb the local structures of imidazolium C—H groups of EMI<sup>+</sup>TFSA<sup>−</sup> and the association configuration is still favored in the presence of 1,4-dioxane. As the pressure is elevated, 1,4-dioxane molecules tend to associate with themselves and TFSA<sup>−</sup> interacts with EMI<sup>+</sup> to form associated configurations. Our results suggest the formation of association between EMI<sup>+</sup> cation and L64 and the complexes are stable up to the pressure of 2.5 GPa.



L64--- EMI<sup>+</sup> TFSA<sup>−</sup>

## I. INTRODUCTION

The ability of block copolymers to form well-defined structures has been the subject of much interest within applied sciences as well as in basic research.<sup>1–6</sup> Triblock PEO-PPO-PEO copolymers, commonly known as Pluronics, are high molecular weight non-ionic surfactants. PEO and PPO denote poly(ethylene oxide) and poly(propylene oxide), respectively. Analogous to small amphiphilic molecules such as lipids and soaps, PEO-PPO-PEO block copolymers are made of hydrophilic PEO blocks and hydrophobic PPO blocks.<sup>1–4</sup> When block copolymers are mixed in a solvent, the middle PPO block tends to form a hydrophobic core and the outer PEO blocks form a hydrophilic corona. The core–corona structures are stabilized by avoiding direct contact between the solvent and the blocks which are insoluble. With hydrophilic PEO blocks and hydrophobic PPO blocks combined into polymer chains, one can obtain copolymer molecules with amphiphilic characteristics which depend critically on parameters like temperature, pressure, and concentration. At low temperature the block copolymers appear as independent chains, i.e., unimers.<sup>1</sup> As the temperature is increased, the PPO block becomes more hydrophobic. This leads to a critical temperature at which micelles are formed.<sup>1</sup> By controlling the architecture of block copolymers, it is possible to generate nanostructures either in an undiluted melt or in solution.<sup>4</sup> The geometries of the copolymers are also related to the volume ratio between insoluble and

soluble blocks, i.e., the insoluble–soluble ratio. The study of interactions between block copolymers and ionic liquids is an exciting emerging area in recent years. For example, block copolymer micelles can transfer from an aqueous phase at room temperature to a hydrophobic ionic liquid at elevated temperature.<sup>7</sup>

Ionic liquids have gained wide attention as a fascinating new class of environmentally friendly alternatives to volatile molecular solvents in recent years.<sup>8–10</sup> In many applications, ionic liquid-based mixtures become more and more important and the properties of ionic liquids can be significantly affected by the presence of other conventional solvents.<sup>8</sup> Studies on ionic liquid/water system revealed the existence of structural organization.<sup>11–13</sup> At high ionic liquid concentrations, ionic liquids seem to form clusters, as in the pure state, and water molecules interact with the cluster without interacting among themselves.<sup>13</sup> Compared to the intensive investigations on the ionic liquid/water mixtures, there have been a few reports on solvation behaviors of ionic liquids in non-aqueous molecular liquids.<sup>14–18</sup> In the present study, we investigate the interactions of ionic liquids with PEO-PPO-PEO block copolymers and 1,4-dioxane.

**Received:** October 7, 2010

**Revised:** December 15, 2010

**Published:** December 29, 2010

There is currently a marked interest in studying aggregates formed by amphiphilic molecules in imidazolium-based ionic liquids.<sup>19–21</sup> The dissolution of some surfactants in ionic liquids depresses the surface tension and this phenomenon indicates the presence of solvophobic interactions in a manner analogous to aqueous solutions. The formation of micelles is possible and the structures of micelles can be tuned by changing the nature of ionic liquids.<sup>19,20</sup> The ability of surfactants to self-aggregate is related to the structure of the surfactant, its concentration, and the solvents.<sup>19</sup> Although the aggregation behaviors of surfactants in ionic liquids have been widely studied, the majority of these studies have paid attention to the surfactant-poor or the ionic liquid-rich composition region. Extreme values of the physical properties exhibited by surfactant/ionic liquid mixtures at the surfactant-rich end of the composition scale have not been observed by various techniques. In our current investigation, we use pressure as a variable to explore the local structures of surfactant/ionic liquid mixtures in the surfactant-rich region. It seems safe to state that surfactant molecules may modify the self-organization pattern of ionic liquids.

Among the interactions taking place in ionic liquids, Coulomb forces between cations and anions are predominant.<sup>9,10</sup> Ionic liquids differ from the classical salts at least in one aspect: they possess hydrogen bonds that induce structural directions.<sup>9</sup> Several physical studies indicate that imidazolium-based ionic liquids possess analogous structural patterns in the solid, liquid, and gas phases. The strongest hydrogen bond involves the most acidic C<sup>2</sup>–H of the imidazolium cation, followed by C<sup>4</sup>–H and C<sup>5</sup>–H. Two or three resolved absorption bands are observed with 1-alkyl-3-methylimidazolium salts in the spectral region between 3000 and 3200 cm<sup>−1</sup>. These can be attributed to coupled aromatic C–H stretching vibrations. In this article, we characterize the local structures of surfactant/ionic liquid mixtures by measuring the spectral features of imidazolium C–H groups.

Application of high pressure is the ideal tool to tune continuously the bonding properties, especially with regard to the interplay of covalent and hydrogen bonding. Changing the temperature of a chemical system produces a simultaneously changes in thermal energy and volume. To separate the thermal and volume effects, one must perform high-pressure experiments. The pressure-induced changes in the vibrational characteristics are of particular interest. Studies have shown the potential significant effect that pressure has on probing the nature of local organizations of ionic liquids.<sup>14,15,22,23</sup> For example, the compression of an EMI<sup>+</sup>TFSA<sup>−</sup>/CD<sub>3</sub>CN mixture leads to the increase in the isolated imidazolium C–H band intensity.<sup>15</sup> Nevertheless, the loss in intensity of the isolated structures was observed for EMI<sup>+</sup>FSA<sup>−</sup>/CD<sub>3</sub>CN mixtures as the pressure was elevated. In other words, the associated configuration is favored for EMI<sup>+</sup>FSA<sup>−</sup>/CD<sub>3</sub>CN mixtures.<sup>15</sup>

## II. EXPERIMENTAL SECTION

Samples were prepared using 1-ethyl-3-methylimidazolium bis(trifluoromethylsulfonyl)amide (EMI<sup>+</sup>TFSA<sup>−</sup>, 98.9%, Fluka), Pluronic L64 (Lot WE19S341/1, Fluka), and 1,4-dioxane (99.9%, Aldrich). Figure 1 shows the schematic diagram of Pluronic L64. Pluronic L64 has the chemical formula EO<sub>13</sub>PO<sub>30</sub>EO<sub>13</sub>, where EO and PO denote ethylene oxide and propylene oxide, respectively. A diamond anvil cell (DAC) of Merrill–Bassett design, having a diamond culet size of 0.6 mm, was used for generating pressures up to ca. 2 GPa. Two type-IIa diamonds were used for mid-infrared measurements. The sample was contained in a

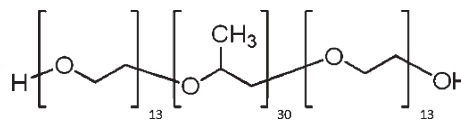
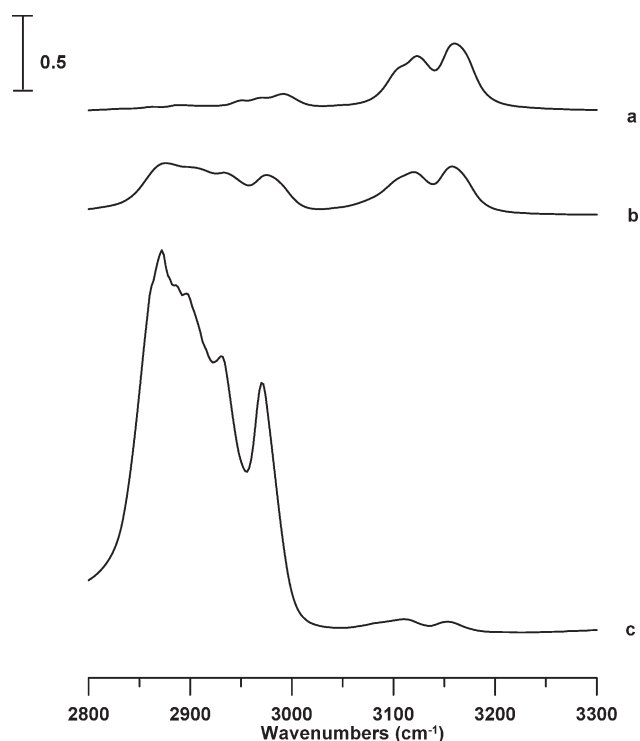


Figure 1. Schematic diagram of Pluronic L64.

0.3 mm diameter hole in a 0.25 mm thick Inconel gasket mounted on the diamond anvil cell. To reduce the absorbance of the samples, CaF<sub>2</sub> crystals (prepared from a CaF<sub>2</sub> optical window) were placed into the holes and compressed firmly prior to inserting the samples. A droplet of a sample filled the empty space of the entire hole of the gasket in the DAC, which was subsequently sealed when the opposed anvils were pushed toward one another. Infrared spectra of the samples were measured on a PerkinElmer Fourier transform spectrophotometer (model Spectrum RXI) equipped with a LITA (lithium tantalite) mid-infrared detector. The infrared beam was condensed through a SX beam condenser onto the sample in the diamond anvil cell. Typically, we chose a resolution of 4 cm<sup>−1</sup> (data point resolution of 2 cm<sup>−1</sup>). For each spectrum, typically 1000 scans were compiled. To remove the absorption of the diamond anvils, the absorption spectra of DAC were measured first and subtracted from those of the samples. Pressure calibration follows Wong's method.<sup>24,25</sup> The spectra of samples measured at ambient pressure were taken by filling samples in a cell having two CaF<sub>2</sub> windows without the spacers.

## III. RESULTS AND DISCUSSION

Figure 2a displays infrared spectra of pure 1-ethyl-3-methylimidazolium bis(trifluoromethylsulfonyl)amide (EMI<sup>+</sup>TFSA<sup>−</sup>) obtained under ambient pressure. The bis(trifluoromethylsulfonyl)amide anion is also called NTf<sub>2</sub><sup>−</sup>, Tf<sub>2</sub>N<sup>−</sup>, and TFSI<sup>−</sup> in the literature. As indicated in Figure 2a, the peaks at the region between 3050 and 3200 cm<sup>−1</sup> are attributed to coupled C–H stretching modes of C<sup>2</sup>–H, C<sup>4</sup>–H, and C<sup>5</sup>–H on the imidazolium cation. We also observed a weak shoulder at approximately 3103 cm<sup>−1</sup> in Figure 2a. The nearly degenerated peaks, i.e., 3103 and 3123 cm<sup>−1</sup>, indicate that the imidazolium C–H may exist in two different forms (isolated and associated structures) and the splitting may be attributed to the perturbation of neighboring ions in the liquid state.<sup>26–28</sup> As can clearly be seen from Figure 2, b and c, the addition of Pluronic L64 to EMI<sup>+</sup>TFSA<sup>−</sup> leads to appreciable changes in band frequencies and shapes of the imidazolium C–H stretching bands. It is well-known that the imidazolium C–H stretching region may be described by two doublets (four bands), one doublet at the lower frequencies is assigned to the C<sup>2</sup>–H stretching modes and another doublet at the higher frequencies is attributed to the coupled C<sup>4</sup>–H and C<sup>5</sup>–H stretching modes.<sup>26</sup> The splitting of the bands in doublets was assigned to the existence in the bulk phase of isolated pairs with stronger hydrogen bonding to the counteranion, in addition to associated ion pairs with weaker hydrogen bonding.<sup>26</sup> As shown by Figure 3, where frequencies of two doublets have been plotted versus weight percent of EMI<sup>+</sup>TFSA<sup>−</sup>, calculated from sample preparation by weight, the decrease in frequencies upon dilution was observed at high concentrations of EMI<sup>+</sup>TFSA<sup>−</sup> (wt % > 30). Previous studies have shown that the shifts of C–H bands are closely related to changes in the liquid structure and solvation states.<sup>22,23,26</sup> Our observations suggest that L64 molecules may be capable of breaking the cation–anion clusters via the interactions between cation and L64 and anion and L64. Looking into more detail in Figure 3, we observe no drastic changes in the



**Figure 2.** IR spectra of pure  $\text{EMI}^+\text{TFSA}^-$  (curve a) and mixtures of  $\text{EMI}^+\text{TFSA}^-/\text{L64}$  with 76 wt %  $\text{EMI}^+\text{TFSA}^-$  (curve b) and 12 wt %  $\text{EMI}^+\text{TFSA}^-$  (curve c).

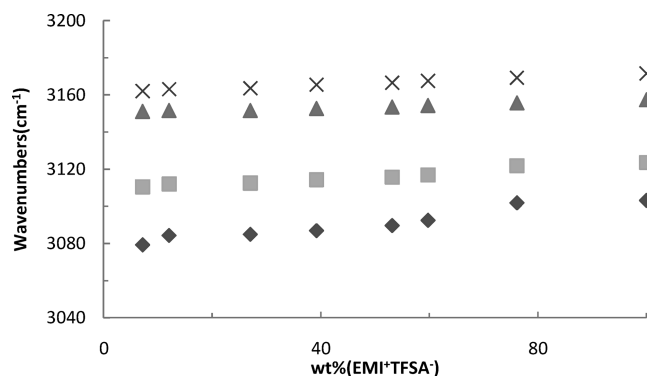


**Figure 3.** Concentration dependence of the imidazolium C–H stretching frequencies of  $\text{EMI}^+\text{TFSA}^-/\text{L64}$  versus the wt % of  $\text{EMI}^+\text{TFSA}^-$ .

concentration dependence of the imidazolium C–H band frequency at low concentrations of  $\text{EMI}^+\text{TFSA}^-$ , that is, wt % ( $\text{EMI}^+\text{TFSA}^-$ ) < 30. These results indicate the formation of a certain solvation structure around  $\text{EMI}^+$  cations in L64-rich regions (wt%( $\text{EMI}^+\text{TFSA}^-$ ) < 30), but much more effort is needed to illustrate the details. We note that the two bands of the doublet at lower frequencies are more concentration sensitive than those of the doublet at higher frequencies as shown in Figure 3. A possible explanation for this effect is the formation of  $\text{C}^2\text{--H}\cdots\text{O}$  interactions between imidazolium  $\text{C}^2\text{--H}$  groups and oxygen atoms of PEOs. As illustrated in Figure 3, the  $\text{C}^2\text{--H}$  and  $\text{C}^{4,5}\text{--H}$  can be involved in hydrogen bonding and the favored approach for oxygen atoms to interact with the imidazolium cation is through the formation of  $\text{C}^2\text{--H}\cdots\text{O}$ . In other words, L64 can be added to change the relative contribution of the isolated and

associated components. The associated species may be larger ion clusters (or ion pairs) and the isolated species may mean the dissociation into smaller ion clusters (or free ions). We notice that significant changes in relative intensities of two doublets occur in Figure 2b,c. As revealed, an increase in the relative intensity of the doublet at lower frequencies was observed in Figure 2c. We also analyzed the relative intensity ( $I_{3103}/I_{3123}$ ) of two components in the lower doublet as shown in Figure S1 (see Supporting Information) and the increase in the relative intensity of the  $3103\text{ cm}^{-1}$  component was found. Evolution of relative band intensities may be related to the equilibrium among free ions, ion pairs, and higher clusters in mixtures of  $\text{EMI}^+\text{TFSA}^-/\text{L64}$ . There are many investigations which report weak hydrogen bondings, such as  $\text{C--H}\cdots\text{O}$  and  $\text{C--H}\cdots\text{X}$ , in the structure of ionic liquids.<sup>9</sup> Nevertheless, experimental evidence of  $\text{C--H}\cdots\text{O}$  and  $\text{C--H}\cdots\text{X}$  is notoriously difficult to obtain. There has been a longstanding discussion on the nature of weak hydrogen bonding, as some spectroscopic behaviors are opposite to those of classical hydrogen bonds.<sup>29,30</sup> Scheiner and Dannenberg found that there are no fundamental differences between weak hydrogen bonding and conventional hydrogen bonding and explain the differences on the basis of a combination of electrostatic, polarization, charge transfer, dispersion, and steric repulsion forces between the proton donors and acceptors.<sup>31,32</sup> Thus, the origin of both the red-shifted and blue-shifted hydrogen bonds may be the same as shown by Schlegel and Hermansson.<sup>33,34</sup> As shown by Figure 3, red shifts in imidazolium C–H frequencies are observed as  $\text{TFSA}^-$  is replaced by L64.

In order to learn the associated-dissociated structures in detail, we have studied pressure-dependent variation in the infrared spectra of  $\text{EMI}^+\text{TFSA}^-/\text{L64}$  mixtures. Figure 4 presents IR spectra of a  $\text{EMI}^+\text{TFSA}^-/\text{L64}$  mixture having its wt % of  $\text{EMI}^+\text{TFSA}^-$  equal to 19 obtained under ambient pressure (curve a) and at 0.3 (curve b), 0.9 (curve c), 1.5 (curve d), 1.9 (curve e), and 2.3 GPa (curve f). As indicated in Figure 4a, the  $2874$  and  $2975\text{ cm}^{-1}$  bands are mainly due to alkyl C–H stretching vibrations of L64 and the bands at the region between  $3050$  and  $3200\text{ cm}^{-1}$  correspond to imidazolium C–H stretching vibrations of  $\text{EMI}^+\text{TFSA}^-$ . As the sample was compressed, that is, increasing the pressure from ambient (Figure 4a) to 0.3 GPa (Figure 4b), the alkyl C–H stretching modes underwent dramatic changes in their spectral profiles as the pressure was elevated to 0.3 GPa in curve b and the alkyl C–H bands were separated to  $2890$ ,  $2932$ , and  $2984\text{ cm}^{-1}$ . This may indicate a pressure-induced transformation upon compression. The phase transition, i.e., sol-to-gel transition or solidification, may occur as the pressure is elevated. The results are in agreement with the fact that the Pluronics show complex phase behaviors by varying the pressure.<sup>1,2,5</sup> The amphiphilic characteristics of triblock copolymers depend critically on thermodynamics parameters like temperature and pressure. This leads to self-assembly into a variety of structures including spherical, rodlike, and pancake-shaped micelles.<sup>1,2,5</sup> The imidazolium C–H bands in Figure 4 display anomalous nonmonotonic pressure-induced frequency shifts. As revealed in Figure 4b, the imidazolium C–H bands were blue-shifted caused by the compression. Further increases in pressure, cf., Figure 4b–d, do not induce significant changes in the absorption frequencies of the imidazolium C–H bands. We also notice that no appreciable changes in the relative band intensities of the imidazolium C–H bands were observed in Figure 4. These results indicate that the isolated configurations caused by the addition of L64 may be still stable under high pressure.

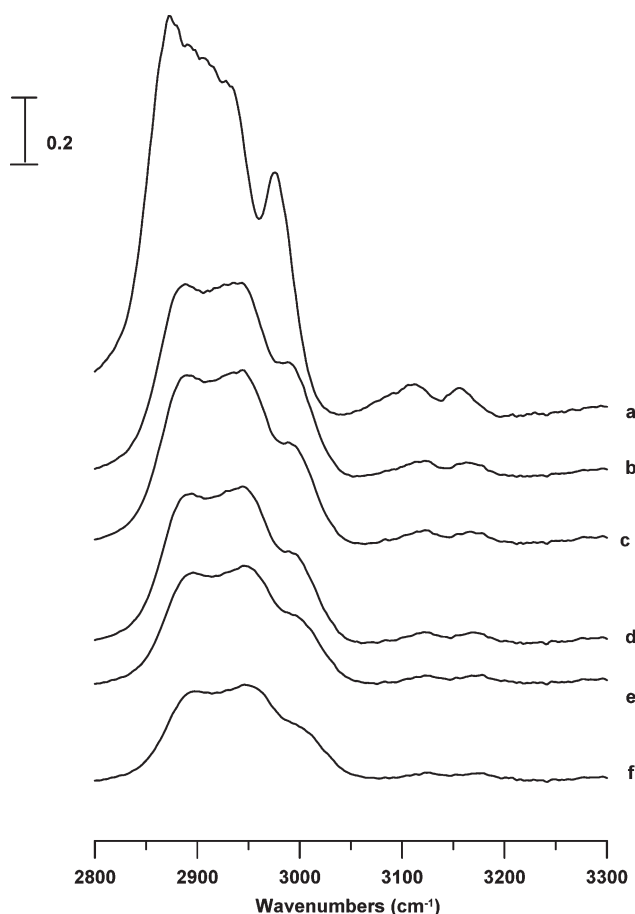


**Figure 4.** IR spectra of a  $\text{EMI}^+\text{TFSA}^-/\text{L64}$  mixture (19 wt %  $\text{EMI}^+\text{TFSA}^-$ ) obtained under ambient pressure (curve a) and at 0.3 (curve b), 0.9 (curve c), 1.5 (curve d), 1.9 (curve e), and 2.3 GPa (curve f).

Figure 5 displays IR spectra of a  $\text{EMI}^+\text{TFSA}^-/\text{1,4-dioxane}$  mixture with 20 wt %  $\text{EMI}^+\text{TFSA}^-$  obtained under ambient pressure (curve a) and at 0.3 (curve b), 0.9 (curve c), 1.5 (curve d), 1.9 (curve e), and 2.3 GPa (curve f). Interactions between 1,4-dioxane and  $\text{EMI}^+\text{TFSA}^-$  are very interesting because a 1,4-dioxane molecule contains two ethylene oxide groups, making it possible to form C—H...O interactions with imidazolium C—H groups of  $\text{EMI}^+\text{TFSA}^-$ . Figure 5a shows that the dilution of  $\text{EMI}^+\text{TFSA}^-$  in the  $\text{EMI}^+\text{TFSA}^-/\text{1,4-dioxane}$  mixture leads to negligible changes in vibrational frequencies and spectral shapes of imidazolium C—Hs by comparing Figures 2a and 5a. On the basis of the results of Figure 5, we found that the oxygen atoms of 1,4-dioxane may not significantly perturb the local structures of imidazolium C—H groups of  $\text{EMI}^+\text{TFSA}^-$ . As revealed in Figure 5, the association configuration is still favored even in the presence of 1,4-dioxane and this result is remarkably different from the spectral changes revealed in the  $\text{EMI}^+\text{TFSA}^-/\text{L64}$  mixture (see Figure 4). Figure 5a in the 2800–3050  $\text{cm}^{-1}$  region exhibits two major absorption bands at 2851 and 2958  $\text{cm}^{-1}$  corresponding to C—H stretching modes of axial C—H and equatorial C—H groups of 1,4-dioxane, respectively.<sup>35</sup> A phase transition, i.e., pressure-induced solidification, was observed in Figure 5b, as the IR spectrum of alkyl C—H stretching modes becomes four separated bands. We anticipate that the spectral features in the alkyl C—H region observed in Figure 5b are attributed to the formation of hydrogen-bond-like C—H...O interactions between neighboring 1,4-dioxane.<sup>35</sup>

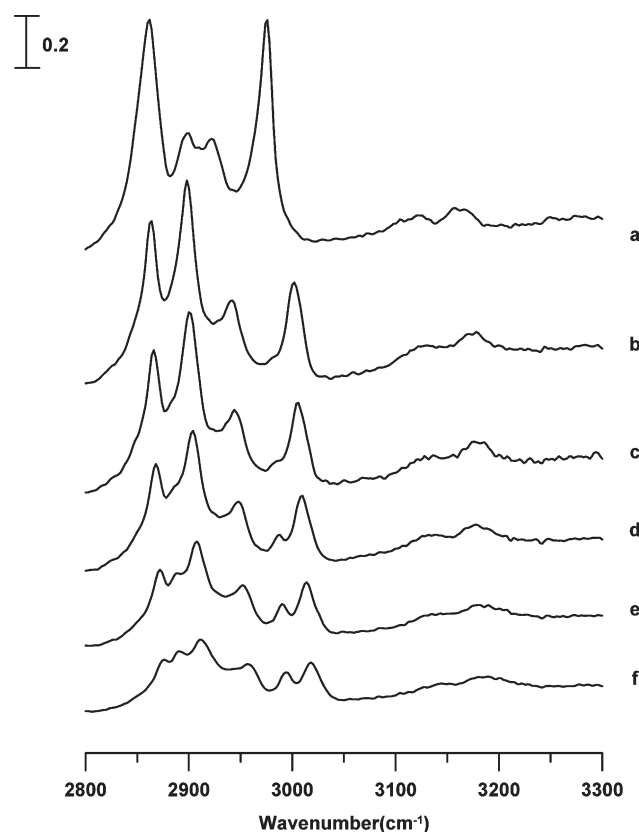


**Figure 5.** IR spectra of a  $\text{EMI}^+\text{TFSA}^-/\text{1,4-dioxane}$  mixture (20 wt %  $\text{EMI}^+\text{TFSA}^-$ ) obtained under ambient pressure (curve a) and at 0.3 (curve b), 0.9 (curve c), 1.5 (curve d), 1.9 (curve e), and 2.3 GPa (curve f).

On the basis of the pressure-dependent results in Figure 5, 1,4-dioxane molecules may prefer to associate with themselves and  $\text{TFSA}^-$  interacts with the cation to form associated configurations under high pressure. A further increase in pressure leads to blue shifts of the alkyl C—H stretching modes in Figure 5b–g. Two new bands at ca. 2891 and 2994  $\text{cm}^{-1}$  appear in Figure 5e,f.

Figure 6 displays the infrared spectra of a  $\text{EMI}^+\text{TFSA}^-/\text{L64}/\text{1,4-dioxane}$  mixture with 20 wt %  $\text{EMI}^+\text{TFSA}^-$ , 40 wt % L64, and 40 wt % 1,4-dioxane, respectively, obtained under ambient pressure (curve a) and at 0.3 (curve b), 0.9 (curve c), 1.5 (curve d), 1.9 (curve e), and 2.3 GPa (curve f). Figure 6a reveals similar imidazolium C—H absorption bands as Figure 4a, i.e., the  $\text{EMI}^+\text{TFSA}^-/\text{L64}$  mixture. Thus, imidazolium C—H spectral features observed in Figure 6a may arise from the interactions between  $\text{EMI}^+\text{TFSA}^-$  and L64. It appears that the imidazolium C—H groups tend to associate with the outer ethylene oxide blocks of L64 instead of ethylene oxide groups of 1,4-dioxane and this observation is in accord with the experimental results revealed in Figures 4 and 5. As the pressure was elevated in Figure 6b–f, imidazolium C—H bands were blue-shifted.

To illustrate the frequency shift, the pressure dependence of imidazolium C—H band frequencies of pure  $\text{EMI}^+\text{TFSA}^-$ ,  $\text{EMI}^+\text{TFSA}^-/\text{1,4-dioxane}$ ,  $\text{EMI}^+\text{TFSA}^-/\text{L64}$ , and  $\text{EMI}^+\text{TFSA}^-/\text{L64}/\text{1,4-dioxane}$  was plotted (the lower doublet shown in Figure 7 and the higher doublet shown in Figure S2 in the Supporting Information). It is interesting to note that the imidazolium C—H bands display anomalous pressure-induced frequency shifts as revealed in Figure 7 and Figure S2. Analysis of the pressure dependence of the imidazolium C—H peaks of pure  $\text{EMI}^+\text{TFSA}^-$



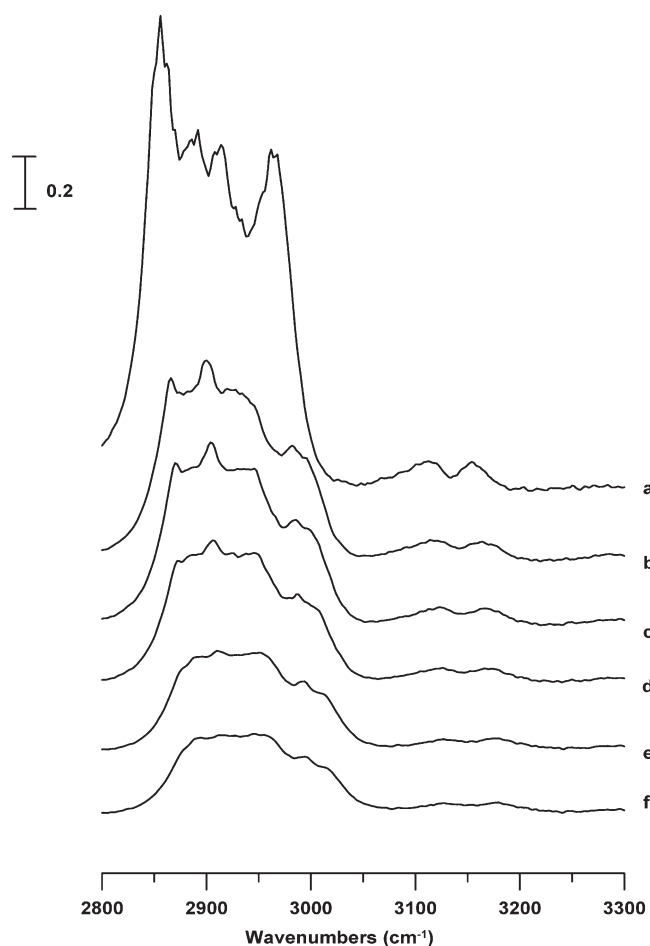


**Figure 6.** IR spectra of a  $\text{EMI}^+\text{TFSA}^-/\text{L64}/1,4\text{-dioxane}$  mixture (20 wt %  $\text{EMI}^+\text{TFSA}^-$ , 40 wt % L64, and 40 wt % 1,4-dioxane) obtained under ambient pressure (curve a) and at 0.3 (curve b), 0.9 (curve c), 1.5 (curve d), 1.9 (curve e), and 2.3 GPa (curve f).

yields blue frequency shifts at pressure below 0.3 GPa, then undergoes no change from 0.3 to 0.9 GPa, and then blue-shifts again upon increasing the pressure ( $p > 1.5$  GPa). This discontinuity in frequency shift is similar to the trend revealed in our previous report of pure 1-butyl-3-methylimidazolium hexafluorophosphate. Inspection of the pressure dependence shows that the  $\text{EMI}^+\text{TFSA}^-/1,4\text{-dioxane}$  mixture (squares in Figure 7 and Figure S2) also displays similar pressure-induced frequency shifts. The similarity between pure  $\text{EMI}^+\text{TFSA}^-$  (Figure 7 and Figure S2) and  $\text{EMI}^+\text{TFSA}^-/1,4\text{-dioxane}$  (Figure 7 and Figure S2) suggests that associated structures are dominant and stable up to the pressure of 2.5 GPa even in the presence of 1,4-dioxane. As the L64 was added, i.e.,  $\text{EMI}^+\text{TFSA}^-/\text{L64}$  and  $\text{EMI}^+\text{TFSA}^-/\text{L64}/1,4\text{-dioxane}$  in Figure 7 and Figure S2, we observed red-shifts in frequency for imidazolium C–H bands under the ambient pressure. The red frequency shifts of the imidazolium C–H modes should be attributed to the local structural reorganization of imidazolium C–H groups by the presence of L64 and our experimental observations support a strong interaction between imidazolium C–H and the oxygen atoms in L64. It is likely that the presence of L64 perturbs the ionic liquid–ionic liquid association in the polar region. As the pressure was elevated, the imidazolium C–H peaks of  $\text{EMI}^+\text{TFSA}^-/\text{L64}$  and  $\text{EMI}^+\text{TFSA}^-/\text{L64}/1,4\text{-dioxane}$  in Figure 7 and Figure S2 display similar frequency

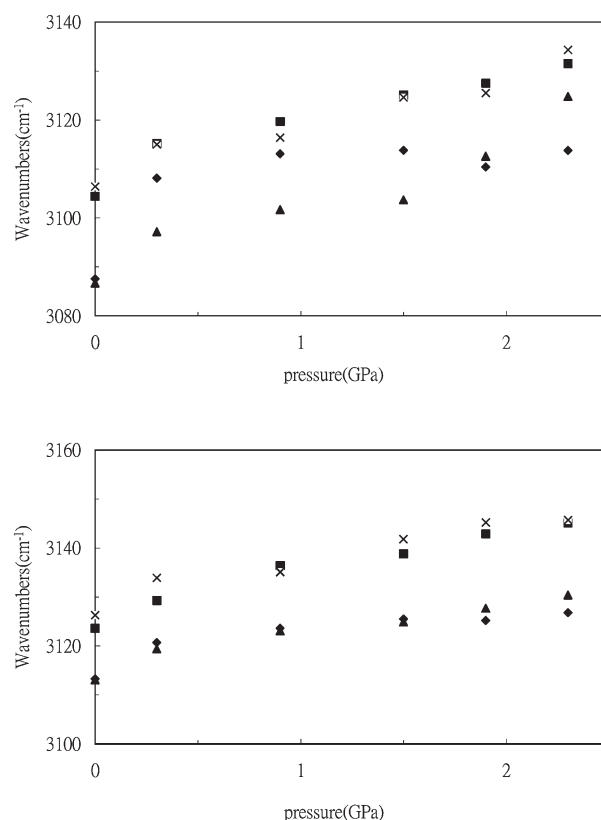


**Figure 7.** Pressure dependence of the imidazolium C–H stretching frequencies of pure  $\text{EMI}^+\text{TFSA}^-$  (x),  $\text{EMI}^+\text{TFSA}^-/1,4\text{-dioxane}$  (■),  $\text{EMI}^+\text{TFSA}^-/\text{L64}$  (◆), and  $\text{EMI}^+\text{TFSA}^-/\text{L64}/1,4\text{-dioxane}$  (▲).

shifts. This observation suggests that L64 has the ability to strongly solvate  $\text{EMI}^+\text{TFSA}^-$ , but 1,4-dioxane cannot form complexes with  $\text{EMI}^+\text{TFSA}^-$ . This fact could be related to the well-known supramolecular complexation between imidazolium salts and macrocycles.<sup>36</sup> For example, it is already known that the imidazolium cation can form inclusion complexes with large crown ether type hosts via hydrogen bonding.<sup>36</sup> In other words, our experimental results provide evidence for the formation of association between  $\text{EMI}^+\text{TFSA}^-$  and L64 via imidazolium C–H...O interactions and the complexes are stable under the condition of high pressure.

#### IV. CONCLUSION

Pressure-dependent behaviors of imidazolium C–H bands in ionic liquid mixtures are found to depend on the isolated and associated structures. For the  $\text{EMI}^+\text{TFSA}^-/\text{L64}$  mixture, L64 molecules are capable of perturbing the cation–anion clusters via the interactions between cation and L64. A possible explanation for this effect is the formation of C–H...O interactions between imidazolium C–H groups and oxygen atoms of PEOs. However, the associated configuration is still favored for  $\text{EMI}^+\text{TFSA}^-/1,4\text{-dioxane}$  mixtures. This observation suggests that L64 has the ability to strongly solvate  $\text{EMI}^+\text{TFSA}^-$ , but 1,4-dioxane cannot form complexes with  $\text{EMI}^+\text{TFSA}^-$ .

#### ■ ASSOCIATED CONTENT

**S Supporting Information.** Concentration dependence of the imidazolium C–H stretching relative intensities of

EMI<sup>+</sup>TFSA<sup>-</sup>/L64 versus the wt % of EMI<sup>+</sup>TFSA<sup>-</sup> (Figure S1) and pressure dependence of the imidazolium C–H stretching frequencies of pure EMI<sup>+</sup>TFSA<sup>-</sup>, EMI<sup>+</sup>TFSA<sup>-</sup>/1,4-dioxane, EMI<sup>+</sup>TFSA<sup>-</sup>/L64, and EMI<sup>+</sup>TFSA<sup>-</sup>/L64/1,4-dioxane (Figure S2). This material is available free of charge via the Internet at <http://pubs.acs.org>.

## AUTHOR INFORMATION

### Corresponding Author

\*E-mail: [hcchang@mail.ndhu.edu.tw](mailto:hcchang@mail.ndhu.edu.tw). Fax: +886-3-8633570. Phone: +886-3-8633585.

## ACKNOWLEDGMENT

The authors thank the National Dong Hwa University and the National Science Council (Contract No. NSC 98-2113-M-259-005-MY3) of Taiwan for financial support. The authors thank Hou-Kuan Li, Yu-Fang Yeh, and Chen-Pin Duang for their assistance.

## REFERENCES

- (1) Mortensen, K. *J. Phys.: Condens. Matter* **1996**, *8*, A103.
- (2) Kostko, A. F.; Harden, J. C.; McHugh, M. A. *Macromolecules* **2009**, *42*, 5328.
- (3) Zhang, S.; Li, N.; Zheng, L.; Li, X.; Gao, Y.; Yu, L. *J. Phys. Chem. B* **2008**, *112*, 10228.
- (4) Smart, T.; Lomas, H.; Massignani, M.; Flores-Merino, M. V.; Perez, L. R.; Battaglia, G. *Nanotoday* **2008**, *3*, 38.
- (5) Kloxin, C. J.; van Zanten, J. H. *Macromolecules* **2010**, *43*, 2084.
- (6) Virgili, J. M.; Nedoma, A. J.; Segalman, R. A.; Balsara, N. P. *Macromolecules* **2010**, *43*, 3750.
- (7) Bai, Z.; Lodge, T. P. *J. Phys. Chem. B* **2009**, *113*, 14151.
- (8) Wasserscheid, P.; Welton, T., Eds. *Ionic Liquids in Synthesis*; Wiley VCH: Weinheim, Germany, 2008.
- (9) Weingartner, H. *Angew. Chem., Int. Ed.* **2008**, *47*, 654.
- (10) Castner, E. W.; Wishart, J. F. *J. Chem. Phys.* **2010**, *132*, 120901.
- (11) Schroder, U.; Wadhawan, J. D.; Compton, R. G.; Marken, F.; Suarez, P. A. Z.; Consorti, C. S.; de Souza, R. F.; Dupont, J. *New J. Chem.* **2000**, *24*, 1009.
- (12) Triolo, A.; Russina, O.; Bleif, H. J.; Di Cola, E. *J. Phys. Chem. B* **2007**, *111*, 4641.
- (13) Jiang, W.; Wang, Y.; Voth, G. A. *J. Phys. Chem. B* **2007**, *111*, 4812.
- (14) Umebayashi, Y.; Jiang, J. C.; Shan, Y. L.; Lin, K. H.; Fujii, K.; Seki, S.; Ishiguro, S.; Lin, S. H.; Chang, H. C. *J. Chem. Phys.* **2009**, *130*, 124503.
- (15) Umebayashi, Y.; Jiang, J. C.; Lin, K. H.; Shan, Y. L.; Fujii, K.; Seki, S.; Ishiguro, S.; Lin, S. H.; Chang, H. C. *J. Chem. Phys.* **2009**, *131*, 234502.
- (16) Sarkar, S.; Pramanik, R.; Ghatak, C.; Setua, P.; Sarkar, N. *J. Phys. Chem. B* **2010**, *114*, 2779.
- (17) Gao, Y.; Zhang, L.; Wang, Y.; Li, H. *J. Phys. Chem. B* **2010**, *114*, 2828.
- (18) Balevicius, V.; Gdaniec, Z.; Aidas, K.; Tamulienė, J. *J. Phys. Chem. A* **2010**, *114*, 5365.
- (19) Behera, K.; Kumar, V.; Pandey, S. *ChemPhysChem* **2010**, *11*, 1044.
- (20) Patrascu, C.; Gauffre, F.; Nallet, F.; Bordes, R.; Oberdisse, J.; de Lauth-Viguerie, N.; Mingotaud, C. *ChemPhysChem* **2006**, *7*, 99.
- (21) Zheng, L.; Guo, C.; Wang, J.; Liang, X.; Chen, S.; Ma, J.; Yang, B.; Jiang, Y.; Liu, H. *J. Phys. Chem. B* **2007**, *111*, 1327.
- (22) Chang, H. C.; Jiang, J. C.; Chang, C. Y.; Su, J. C.; Hung, C. H.; Liou, Y. C.; Lin, S. H. *J. Phys. Chem. B* **2008**, *112*, 4351.
- (23) Chang, H. C.; Jiang, J. C.; Su, J. C.; Chang, C. Y.; Lin, S. H. *J. Phys. Chem. A* **2007**, *111*, 9201.
- (24) Wong, P. T. T.; Moffatt, D. J.; Baudais, F. L. *Appl. Spectrosc.* **1985**, *39*, 733.
- (25) Wong, P. T. T.; Moffatt, D. J. *Appl. Spectrosc.* **1987**, *41*, 1070.
- (26) Koddermann, T.; Wertz, C.; Heintz, A.; Ludwig, R. *ChemPhysChem* **2006**, *7*, 1944.
- (27) Kotoh, R.; Hara, M.; Tsuzuki, S. *J. Phys. Chem. B* **2008**, *112*, 15426.
- (28) Balasubramanian, S.; Raju, S. G. *J. Phys. Chem. B* **2009**, *113*, 4799.
- (29) Scheiner, S.; Kar, T.; Pattanayak, J. *J. Am. Chem. Soc.* **2002**, *124*, 13257.
- (30) Jablonski, M.; Sadlej, A. J. *Chem. Phys. Lett.* **2008**, *463*, 322.
- (31) Gu, Y. L.; Kar, T.; Scheiner, S. *J. Am. Chem. Soc.* **1999**, *121*, 9411.
- (32) Masunov, A.; Dannenberg, J. J.; Contreras, R. W. *J. Phys. Chem. A* **2001**, *105*, 4737.
- (33) Li, X.; Liu, L.; Schlegel, H. B. *J. Am. Chem. Soc.* **2002**, *124*, 9639.
- (34) Hermansson, K. *J. Phys. Chem. A* **2002**, *106*, 4695.
- (35) Chang, H. C.; Jiang, J. C.; Chuang, C. W.; Lin, S. H. *Chem. Phys. Lett.* **2004**, *397*, 205.
- (36) Noujeim, N.; Leclercq, L.; Schmitzer, A. R. *Curr. Org. Chem.* **2010**, *14*, 1500.